POLİTEKNİK DERGİSİ

JOURNAL of POLYTECHNIC

ISSN: 1302-0900 (PRINT), ISSN: 2147-9429 (ONLINE)
URL: http://dergipark.gov.tr/politeknik

XRD vs Raman for InGaN/GaN structures

InGaN/GaN yapılar için XRD-Raman karşılaştırması

***Yazar(lar) (Author(s))**: Ahmet Kürşat BİLGİLİ[1], Ömer AKPINAR[2], Mustafa Kemal ÖZTÜRK[3], Süleyman ÖZÇELİK[4], Ekmel ÖZBAY[5]*

ORCID[1]: 0000-0003-3420-4936

ORCID[2]: 0000-0002-5172-8283

ORCID[3]: 0000-0002-8508-5714

ORCID[4]: 0000-0002-3761-3711

ORCID[5]: 0000-0003-2953-1828

Bu makaleye şu şekilde atıfta bulunabilirsiniz (To cite to this article): Bilgili A. K., Akpınar Ö., Öztürk M. K., Özçelik S., Özbay E.“ XRD vs Raman for InGaN/GaN structures”, ***Politeknik Dergisi***, 23(2): 291-296, (2020).

Erişim linki (To link to this article): http://dergipark.gov.tr/politeknik/archive

DOI: **10.2339/politeknik.537733**

XRD vs Raman for InGaN/GaN Structures

Research Article / Araştırma Makalesi

Ahmet Kürşat BİLGİLİ[1*], Ömer AKPINAR[1], Mustafa Kemal ÖZTÜRK[1], Süleyman ÖZÇELİK[1], Ekmel ÖZBAY[2]

[1]Gazi University, Photonics Research Center, Ankara/Turkey
[2]Bilkent University, Physics Department, Ankara/Turkey

(Geliş/Received : 03.03.2019 ; Kabul/Accepted : 04.04.2019)

ABSTRACT

In this study, InGaN/GaN structures are grown by using Metal Organic Chemical Vapor Deposition (MOCVD) technique. Some structural, optical and morphological properties of InGaN/GaN structures are investigated in detail. For structural analysis, X-ray diffraction (XRD), for optical, Raman and morphological, Atomic Force Microscopy (AFM) measurement techniques are used. In XRD analysis both samples presented hexagonal crystal structure. XRD peaks for these two samples showed small differences dependent on growth conditions. Strain and stress values are determined from XRD and they are compared with Raman results. In Raman analysis, five different chemicals are determined in both samples. Raman analysis results are in good accordance with XRD, growth conditions and AFM images. In AFM images, there can be seen hills and holes and they are partly homogeneous. There are also some white regions in AFM images. According to Raman peak center data, these white regions are detected as white rust.

Keywords: XRD, InGaN, GaN, MOCVD, AFM, raman.

InGaN/GaN Yapılar için XRD-Raman Karşılaştırması

ÖZ

Bu çalışmada, InGaN/GaN yapılar Metal Organik Kimyasal Buhar Biriktirme (MOCVD) yöntemiyle büyütülmüştür. Bu InGaN/GaN yapıların bazı yapısal, optik ve morfolojik özellikleri detaylı olarak incelenmiştir. Yapısal analiz için X-ışınları kırınımı (XRD), optik özellikler için Raman ve morfolojik özellikler için Atomik Kuvvet Mikroskobu (AFM) kullanılmıştır. XRD analizine göre her iki örnek altıgensel yapı sergilemiştir. Bu iki örnek için elde edilen XRD pikleri büyütme şartlarına bağlı olarak küçük farklılıklar göstermiştir. Gerilme ve stress değerleri XRD den elde edilip Raman sonuçlarıyla kıyaslanmıştır. Raman analizinde, her iki örnekte beş farklı kimyasal tespit edilmiştir. Raman analizi sonuçları XRD ile büyütme koşulları ile ve AFM görüntüleriyle iyi bir uyum içindedir. AFM görüntülerinde tepeler ve çukurlar görülebilir ve bunlar kısmen homojendir. AFM görüntülerinde bir de beyaz bölgeler vardır. Raman pik merkezi verilerine göre bu beyaz bölgeler Beyaz Pastır.

Anahtar Kelimeler: XRD, InGaN, GaN, MOCVD, AFM, raman.

1. INTRODUCTION

Semiconductor nitrites such as GaN and InGaN have a potential use area in optoelectronic and electronic industry because of their physical properties. Both semiconductor structures are in hexagonal shape in thermodynamic equilibrium. GaN and InGaN are binary and triple compounds of nitrite based semiconductors. They have a wide energy band gap range in electromagnetic spectrum. This range changes from near-infrared to ultraviolet region (0.7-6.2 eV) [1].

This property makes nitrite based semiconductors important in designing optoelectronic devices such as light emitting diodes (LEDs), laser diodes, ultraviolet (UV) photodetectors and solar cells. Also, nitrite based semiconductors can operate at high power, frequency and temperature [2].

Although there are some important improvements in optoelectronic device technology containing $In_xGa_{1-x}N$ in their active layers, there are still some uncertainties about the fundamental physics of these structures. Because some physical and chemical properties of InGaN (band gap, lattice parameters, and elastic coefficients) can not be determined accurately, it is also not possible to determine some optical and structural properties certainly. It is known that these parameters for InGaN alloys are strongly dependent on growth conditions [3-4]. A small variation in growth conditions may cause a great quality difference in InGaN thin films. Lee and co-workers showed that if growth speed is decreased the threatening dislocation density decrease 100 times less than the previous value in InGaN/GaN quantum wells [5]. In order to make such materials more common in use and improve them, optimization of production and fabrication should be made. The operation mechanism of them should be understood well. The importance of this study is that stress is calculated from Raman spectra and compared with XRD stress measurements.

*Sorumlu Yazar (Corresponding Author)
e-posta : ahmet.kursat.bilgili@gazi.edu.tr

2. MATERIAL and METHOD

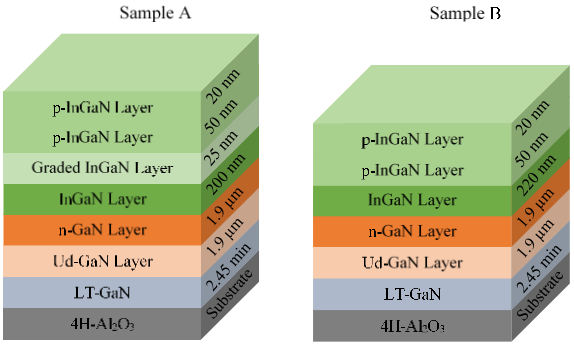

Figure 1. Schematic diagram of (a) S.A and (b) S.B.

InGaN/GaN structures are grown on c-oriented sapphire (Al_2O_3) substrate by using the MOCVD technique. Before growth procedure, in order to remove dirty on the surface of the epitaxial films, they are cleaned at 1100 ^oC under H_2 atmosphere for 10 minutes. After the cleaning process is finished, epitaxial growth operation started with growth of GaN nucleation layer at 575 ^oC [6-7]. During this growth operation, TMGa (*Trimethilgallium*) flow rate, NH_3 flow rate and growth pressure are adjusted as 10 sccm, 1500 sccm and 200 mbar respectively. The thickness of this nucleation layer is 10 nm. After the growth of this layer, GaN buffer layer is grown on it at 1070 ^oC. During the growth of this buffer layer, TMGa flow rate, NH_3 flow rate and growth pressure are adjusted as 15 sccm, 1800 sccm and 200 mbar, respectively. p-type doped InGaN layer is grown by using Mg doping source. The flow rate of this source is 35 sccm. During the growth of InGaN layer, the sources which were on during growth of other layers are kept off. In order to make more doping, Mg flow rate is kept at 40 sccm. Figure.1 (a) and (b) illustrates the schematic diagrams of sample A (S.A) and sample B (S.B).

The thickness of GaN buffer layer is 1.6 µm. Growth procedure continued by opening the SiH_4 source and with the help of this source n-type GaN layer is grown. Flow rate of this layer is 10 sccm. $In_xGa_{(1-x)}N$ active layers are grown at 745 ^oC with 75 sccm In flow rate. Active layers are grown between 1.9 µm n-type GaN and p-type InGaN contact layers.

3. RESULTS and DISCUSSION

In this study, parameters such as dislocation density and stress are estimated by using HR-XRD technique. It is found that dislocation density is high both in S.A and S.B. So peak intensity ratio is used to determine amount of chemicals from Raman spectra instead of peak area ratio. Also, stress measurement results are compared between XRD and Raman. It is known that **XRD** analysis gives more accurate results for stress [8]. Also in Raman spectra very dense white rust peaks are detected. These white rust can be seen in AFM images.

3.1. XRD analysis

Compounds and alloys such as GaN and InGaN have hexagonal structure. Crystal quality of them can be measured by broadening of symmetric peaks. In such layers broadening of rocking curves is maintained by variation of lateral crystal dimensions parallel to wafer surface and tilt angles [9]. HR-XRD omega peaks are given in Figure 2 (a) and (b).

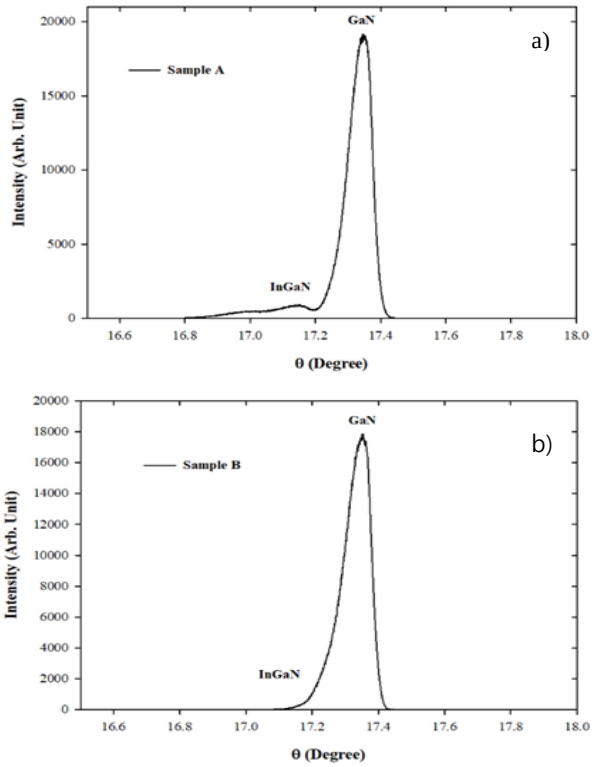

Figure 2. HR-XRD omega peaks for S.A and S.B.

The Full Width at Half Maximum (FWHM) values are given in Table 1. If measured values are compared it is seen that both samples have similar FWHM values for GaN but InGaN layer in S.A has smaller FWHM value than S.B. This result indicates that S.A has a better crystal quality [10].

Table 1. Peak positions and FWHM values for GaN and InGaN layers.

	S.A	**S.B**
FWHM GaN(002)	0.1	0.103
FWHM InGaN(002)	0.166	0.175
Peak position GaN(101)	18.47	18.26
Peak position InGaN(002)	16.92	17.13

3.1.1 Dislocations

A method for calculating lateral and screw type dislocations is dependent on Burgers vector. Metzger and co-workers showed that [11] Burgers vector of mean tilt

angle b=1/3<11-20> is related with lateral type dislocations and Burgers vector of mean tilt angle b=<0001> is related with screw type dislocations. Dislocation density can be calculated with equation (1) [12-13]. Burgers vector is the same with lattice parameters.

$$D_{screw} = \frac{\beta^2_{(0002)}}{9b^2_{screw}}, \quad D_{edge} = \frac{\beta^2_{(10-12)}}{9b^2_{edge}} \qquad (1)$$

β in equation (1) is the FWHM value, b is the Burgers vector. For GaN layer b_{screw}=0.5185 nm, b_{edge}=0.3189 nm. For InGaN layer b_{screw}=0.5198 nm, b_{edge}=0.3417 nm [14].

Table 2. Edge and screw type dislocation density values for S.A and S.B

	S.A		***S.B***	
	Edge ***(D.Lx10^9)***	***Screw*** ***(D.Lx10^8)***	***Edge*** ***(D.Lx10^9)***	***Screw*** ***(D.Lx10^8)***
GaN	1.55	1.25	2.36	1.25
InGaN$_1$	9.55	1.64	10.80	9.55
InGaN$_2$	10.80	1.60	42.90	3.62

3.1.2 Stress from XRD

It is possible to determine stress by using strain measurements [15]. Strain (ε_a) is given with stress in equation (2).

$$\varepsilon_a = \frac{\sigma^*(1-\upsilon)}{E} \qquad (2)$$

Here ε_a is the strain, σ* is stress, υ is Poisson's ratio and E is Young modulus [16]. ε_a value in equation (2) can be determined by plotting sinθ versus βcosθ. Here β is the FWHM value. This plot is shown in Figure.3. Tilt of the fits in this plot gives ε_a. Young modulus is taken as 305 and Poisson's ratio is taken as 0.183 in this study. Strain and stress values are determined as -0.0015, -0.5599 for S.A and -0.0016, -0.5973 for S.B in GPa.

3.2 Raman Analysis

Raman scattering occurs when light interacts with molecular vibrations. This resembles infrared absorption spectroscopy but it has some different properties. The first step to gain Raman spectra is to send a monochromatic beam, like laser, to the sample. Energy of most of the photons forming this beam does not change. This situation is called Rayleigh scattering.

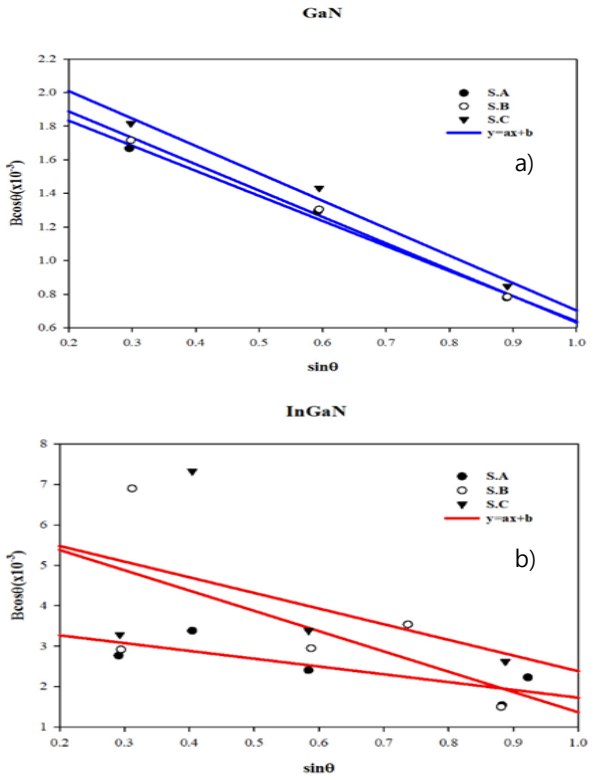

Figure 3. Sinθ versus βcosθ plot for GaN and InGaN layers

1/10x10^6 photons lose their energy or gain more energy. This situation is called Raman scattering. The reason for this Raman shift is interaction of photons with molecular vibrations. The situation that photons lost energy is called STOKES and the situation they gained energy is called ANTI-STOKES. The variation on the energy of sent photons is dependent on the vibrational frequency of the molecules. If vibration is fast (high frequency) it means light atoms are connected each other with strong bonds. In this situation energy variation is important. If vibration is slow (low frequency), it means heavy atoms are connected with weak bonds. In this situation energy variation is small.

In infrared spectroscopy, absorption in infrared region excites vibration and rolling levels of the molecules. Energy of the photons in infrared region is not sufficient for destroying bonds of molecules and they also do not make electronic excitation. But infrared photons can increase amplitude of the vibrations dependent on the molecular geometry and strength of bonds. For Raman Effect a molecular polarization variation during vibration is needed [17].

In this study, for gaining Raman spectra imaging (micro publisher 5.0 RTV) Raman spectrometer is used. Both samples are scanned with 785 nm. Wavelength laser for a duration of 60 s. Raman spectra for S.A and S.B are presented in Figure.4

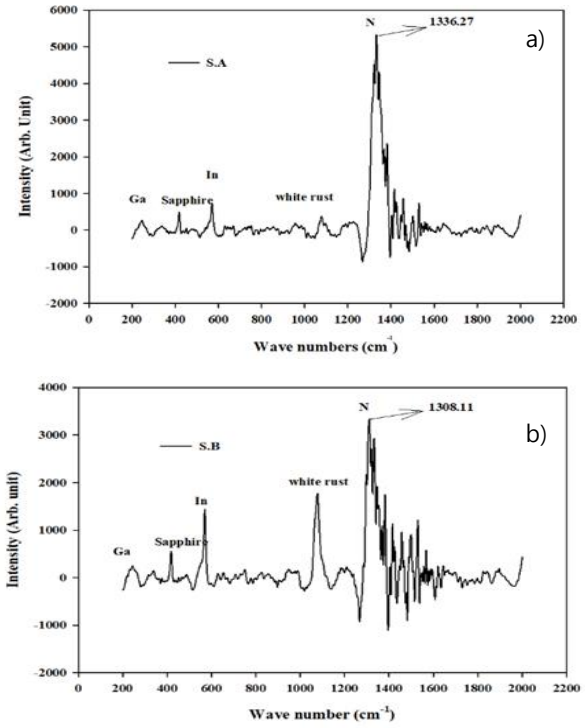

Figure 4. Raman spectras for S.A and S.B

As in the previous sections of this study, identification of material, stress and particle size can be estimated by using Raman spectra. Raman spectroscopy data presented some important knowledge about InGaN/GaN structure. Peak center, peak height, peak area and FWHM values are presented in Table.3 for Ga, N, In and Sapphire. Also one more layer is detected in Raman spectra. That is white rust formed by touching air for a long time.

As can be seen in Table.3 peak intensity ratio and peak area ratios are calculated to estimate amount of materials in the samples. Because dislocation density is high, as shown in XRD section, peak intensity ratio is a more trustable result for amount of materials in percentage. FWHM values in Raman are related with particle size. It is possible to calculate atomic radius of single atoms by using equation (3) [18].

$$r = r_0 . A^{1/3} \tag{3}$$

Here r_0 is coefficient approximately taken as 1.2 fm, A is atomic number in periodic table and r is the atomic radius. Atomic radius of Ga and N are compared with FWHM values in Table.3 gained from Raman analysis. As can be seen they are in good agreement. The order of atomic numbers for N and Ga are, Ga>N and FWHM values for them are like Ga>N. If Table.3 is examined carefully FWHM values for S.A are generally bigger than the ones for S.B. This result also indicates that crystal quality is better in S.A.

Also stress values are calculated from Raman spectra. It is possible to look up the unstressed peak center values for the materials mentioned above from RRUFF database. If these values are subtracted from experimental values and divided by calibration constants we gain stress in MPa. The formula showing this relation is given in equation (4) [19].

$$\sigma(MPa) = \Delta w(cm^{-1}) \tag{4}$$

Comparison of stress values gained from XRD and Raman is made in Table.4. Calculation of stress is made by using N peak center values because it is the most intense peak in both samples.

As can be seen in Table.4 there is great difference in the results gained from XRD and Raman. Because of the physics of Raman scattering it can not detect wafer bending or dislocations, so here XRD results are more trustable. Minus sign in stress values indicate that there is compressive stress in the structure.

Table 4. Comparison of stress values from Raman and XRD.

	S.A	***S.B***
Stress from XRD(MPa)	-559.9	-597.3
Stress from Raman(MPa)	1.017	-5.69

As mentioned above there is one more layer detected by Raman spectroscopy in the samples. That is white rust ($3Zn(OH)_2ZnCO_3H_2O$). White rust is formed over the samples by touching the air for a long time. Peak intensity of white rust is less in S.A.

Table 3. Raman analysis data for S.A and S.B

	S.A					***S.B***				
	Ga	Al_2O_3	In	N	White rust	Ga	Al_2O_3	In	N	White rust
Peak Center	244	419	571	1336.27	1078	244	419	571	1308.11	1078
Peak Area Ratio(%)	3.28	1.95	8.20	17.60	3.24	3.21	2.62	9.47	17.39	6.92
Peak Height Ratio(%)	2.22	5.83	10.74	76.03	5.16	5.82	7.98	18.89	45.53	21.76
FWHM	34.09	8.91	12.48	26.69	xxxx	33.83	9.54	10.65	25.37	xxxx

The reason for this is cleaning procedure of the samples for different durations.

3.3 AFM

In epitaxial structures, difference of the layers may cause great topographic variations on the surface of the samples [20]. For this reason surface morphology of the samples are investigated with AFM. Surface images of the samples are taken with Omicron VT STM/AFM device. Scanning of the surfaces is made in an area of 5x5 μm^2. In Figure.5 AFM images of S.A and S.B are shown. It is obvious in the images that surface morphology of the samples are quite different from each other. On the surface of both samples pits are seen. This is a typical situation for InGaN based hetero structures. On the surface of S.A pits are dominant but on S.B hillocks are dominant. This is related with diffusion of island atoms.

On the other hand roughness is a kind of surface defect. There are many parameters in determining roughness [21]. Root Mean Square (RMS) is the most common parameter to determine surface roughness. For samples A and B RMS values are measured as 2.23 and 4.87. Chen and co-workers reported that In vacancy islands on the surface of the samples or ordered vacancy rows caused lateral segregation [22]. The surface roughness of the samples may be attributed to In segregation and white rust [23]. White rust can be seen on the surface of both samples in AFM images.

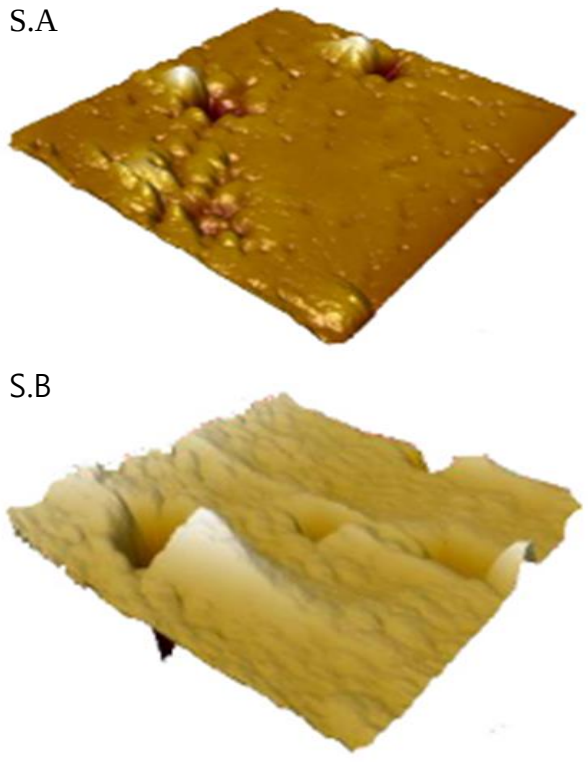

Figure 5. AFM images of S.A and S.B

4. CONCLUSION

In this study, InGaN/GaN structures grown by MOCVD technique on sapphire are investigated in detail by using HR-XRD and Raman spectroscopy. Dislocations are determined with XRD method in order to show dislocation density is high. According to this result peak intensity ratio is more valid than peak area ratio in Raman. Strain and stress values are determined from XRD method and stress values are compared with the ones gained from Raman. Because Raman spectra does not take into account dislocations and wafer bending, values gained from XRD for stress are more valid. All the data gained from Raman spectra are presented in Table.3. Except from the stress and amount of chemicals in the samples, there is one more important result gained from Raman spectra. That is white rust formed over the samples by touching the air for a long time. These white rust can be seen in AFM images clearly. FWHM values gained from Raman spectra are in fact related with crystallite, therefore particle size also effects it. Particle size for single atoms are compared with each other related with FWHM. This study is important because XRD analysis does not show white rust peaks clearly but Raman spectra shows them clearly. Also it is rare in literature to calculate stress from Raman spectra. Stress from XRD is more common in literature.

ACKNOWLEDGEMENTS

This work was supported by the Presidency Strategy and Budget Directorate (Grants Numbers: 2016K121220).

REFERENCES

[1] Huang C.F., Hsieh W.Y., Hsieh B.C., Hsieh C.H. and Lin C.F., "Characterization of InGaN-based photovoltaic devices by varying the indium contents", ***Thin Solid Films***, 529: 278-281, (2013).

[2] Neudeck P.G., R.S Okojie. and L.Y. Chen., "High-temperature electronics - A role for wide bandgap semiconductors", ***Proceedings of the Ieee***, 90(6): 1065-1076, (2002).

[3] Monemar B, Paskov P.P. and Kasic A., "Optical properties of InN—the bandgap question", ***Supperlatt. Microstruct***, 38, (2005).

[4] Nanishi Y., Saito Y. and Yamaguchi T., "RF-Molecular Beam Epitaxy Growth and Properties of InN and Related Alloys", ***Japan J. Appl. Phys,*** 42: 2549, (2003).

[5] Lee S.N., Tan N., Lee W., Paek H., Seon M., Lee I.H., Nam O. and Park Y., "Characterization of optical and crystal qualities in InxGa1–xN/InyGa1–yN multi-quantum wells grown by MOCVD", ***J. Cryst. Growth***, 250: 256, (2003).

[6] Lafont U., Zeijl H. and Zwaag S., " Increasing the reliability of solid state lighting system via self-healing approaches", ***Microelectronic Reliability***, 52(1): 71- 89, (2012).

[7] Akpinar., O., Bilgili A.K., Öztürk M.K., Özçelik S. and Özbay E., "On the elastic properties of INGAN/GAN LED structures", ***Applied Physics a-Materials Science & Processing***, 125(2): (2019).

[8] Oura K., Lifshitsi V.G., Saranin A.A., Zotov A.V. and M. Katayama., "Surface science (First edition)", ***Berlin: Springer*** 166 (229): 378-382, (2003).

[9] Arulkumaran S., Egawa T., Ishikawa H. and Jimb T., "Characterization of different-Al-content $Al_xGa_{1-x}N$/GaN hetrostructures and high-electron-mobility transistors on sapphire", ***Journal of Vacuum Science & Technology***, 21(2): 888-894, (2003).

[10] Akasaki I. and Amano H., "Breakthroughs in Improving Crystal Quality of GaN and Invention of the p-n Junction Blue-Light-Emitting Diode", ***Japanese Journal of Applied Physics***, 47(5): 3781-3781, (2008).

[11] Ambacher O., " Growth and applications of Group III-nitrides", ***Journal of Applied***, 31(1): 2653–2710, (1998).

[12] Vickers M.E., Kappers M.J., Datta R., McAleese C., Smeeton T.M., Rayment F.D.G. and Humphreys C.J.," In-plane imperfections in GaN studied by x-ray diffraction", ***Journal of Physics D***: ***Applied Physics***, 38(A10): A99-A104, (2006).

[13] Moram M.A. and Vickers M.E., "X-ray diffraction of III-nitrides", ***Reports on Progress in Physics***, 72(3): (2009).

[14] Yu H., Ozturk M.K., Ozcelik S. and Ozbay E.,"MOCVD growth and optical properties of non-polar (11-20) a-plane GaN on (10-12)r-plane sapphire substrate", ***J. Cryst. Growth*** , 293: 273, (2006).

[15] Harutyunyan V.S., Aivazyan A.P., Weber E.R., Kim Y., Park Y. and Subramanya S.G.," High resolution x-ray diffraction strain-stress analysis of GaN/Sapphire heterostructures", ***Journal of Physics D: Applied Physics***, 34(10A): A35-A39, (2009).

[16] Halliwell M.A.G., "X-ray diffraction solutions to heteroepitaxial growth problems", ***Journal of Crystal Growth***, 170(1-4): 47-54, (1997).

[17] Xu H.X., Bjerneld J., Kall M. And Börjesso L.," Spectroscopy of single hemoglobin molecules by surface enhanced Raman scattering", ***Physical Review Letters***, 83(21): 4357-4360, (1999).

[18] Heilig K., "Changes in Mean-Square Nuclear-Charge Radii from Optical Isotope Shifts of Long Chains of Isotopes", ***Hyperfine Interactions***, 24(1-4): 349-375, (1985).

[19] C.P. Constable, Lewis D.B., Yarwood J. And Münz W.D.," Raman microscopic studies of residual and applied stress in PVD hard ceramic coatings and correlation with X-ray diffraction (XRD) measurements", ***Surface & Coatings Technology***, 184(2-3): 291-297, (2004).

[20] Yıldız A., Öztürk M.K., Bosi M., Özçelik S. and M. Kasap," Structural, electrical and optical characterization of InGaN layers grown by MOVPE", ***Chinese Physics B***, 18(9): 4007-4012, (2009).

[21] Dunn C.G., Kogh E.F., "Comparison of dislocation densities of primary and secondary recrystallization grains of Si-Fe", ***Acta Metallurgica***, 5(10): 548-554, (1957).

[22] Tao T., Zhao Z., Lian L., Hui S., Zili X., Rong Z., Bin L., Xiangqian X., Li Y., Ping H., Yi S. and Youdou Z., "Surface morphology and composition studies in InGaN/GaN film grown by MOCVD", ***Journal of Semiconductors***, 32(8): 1-3, (2011).

[23] Çörekçi S., Öztürk M.K., Akaoğlu B., Çakmak M., Özçelik S. and Özbay E., "Structural, morphological, and optical properties of AlGaN/GaN heterostructures with AlN buffer and interlayer", ***Jour***